

UC Berkeley

UC Berkeley Previously Published Works

Title

The structure of ambient water

Permalink

<https://escholarship.org/uc/item/1j23x6rm>

Journal

Molecular Physics, 108(11)

ISSN

0026-8976

Authors

Clark, Gary NI
Cappa, Christopher D
Smith, Jared D
[et al.](#)

Publication Date

2010-06-10

DOI

10.1080/00268971003762134

Peer reviewed

The Structure of Ambient Water

Gary N. I. Clark¹, Christopher D. Cappa², Jared D. Smith³
Richard J. Saykally^{3,5}, Teresa Head-Gordon^{1,4*}

¹*Department of Bioengineering, University of California, Berkeley
Berkeley, California 94720 USA*

²*Department of Civil & Environmental Engineering, University of California, Davis
Davis, California 95616 USA*

³*Chemical Sciences Division and* ⁴*Physical Biosciences Division,
Lawrence Berkeley National Laboratory, Berkeley, California 94720 USA*

⁵*Department of Chemistry, University of California, Berkeley
Berkeley, California 94720 USA*

We review the spectroscopic techniques and scattering experiments used to probe the structure of water, and their interpretation using empirical and *ab initio* models, over the last 5 years. We show that all available scientific evidence overwhelmingly favors the view of classifying water near ambient conditions as a uniform, continuous tetrahedral liquid. While there are controversial issues in our understanding of water in the supercooled state, in confinement, at interfaces, or in solution, there is no real controversy in what is understood as regards bulk liquid water under ambient conditions.

*Corresponding author:
*Stanley Hall 274
510-666-2744 (V)
TLHead-Gordon@lbl.gov*

1. INTRODUCTION

The unusual properties of water continue to haunt us in developing a unified understanding of the physical behavior of common, everyday liquids. D. H. Lawrence's quote¹

Water is H₂O, hydrogen two parts, and oxygen one
But there is also a third thing, that makes it water
And no one knows what that is
(I believe God knows)

emphasizes a primal view of the centrality of water to life, at least as we know it on earth.

For mere mortals it is the subject of a wide number of topical reviews²⁻⁹ that cover its properties over the extreme regions of its phase diagram where many questions remain open, as well as at ambient temperatures where its behavior is much better understood. Of all possible properties, liquid water structure is an important organizing framework for understanding water's thermodynamic and kinetic anomalies¹⁰⁻¹³. Starting from the pioneering work of Bernal over 75 years ago¹⁴, it has long been accepted that the structure of liquid water under ambient conditions is, on average, tetrahedral, although the thermal motion in the liquid causes expected distortions from the crystalline structure of ice.¹⁵

Periodically this structural view of liquid water is challenged based on new experiments or preparations that claim to have discovered completely new and dominant hydrogen-bonded network structures of water. The most infamous example was the reported discovery of polywater¹⁶ in the 1960's by scientists who forced water through narrow quartz capillary tubes, to yield what was then claimed as a new form of water, with a lower freezing point and a higher boiling point, and with a density that was ~20% greater than normal water. Controversy raged for ~5 years during which scientists around the world debated the quality or plausibility of the original experiments¹⁷⁻¹⁹, while some claimed to have reproduced polywater in their own labs^{20, 21}, and theorists put forth explanations to its structure and molecular origins²²⁻²⁵. The public became concerned with the possibility of a doomsday scenario of polymerization of vital water supplies if the new form of water came in contact with normal water^{21, 26}, similar to the satirical scenario anticipated by Kurt Vonnegut in the science fiction novel *Cat's Cradle*²⁷. One of the emergent structural models of the polywater liquid²¹ thought to be consistent with infrared (IR) and Raman

spectra, involved highly branched polymer chains of water molecules (Figure 1). Finally, researchers using electron and infrared spectroscopy successfully ended the controversy in 1970 by showing that salt contaminants, primarily sodium lactate found in human sweat, were responsible for the spectral features that were claimed to be unique to polywater.^{19, 28, 29}

The most recent challenge to “orthodoxy” of water structure claims, again, that water is not a uniform tetrahedral liquid, but instead arranges its network into strongly hydrogen bonded chains or rings embedded in a disordered cluster network connected mainly by weak hydrogen bonds³⁰. Recent X-ray absorption and Raman spectroscopy (XAS and XRS) experiments^{30, 31} conducted by Nilsson and co-workers, and a number of corresponding theoretical studies modelling core electron excitations that are central to the XAS experiment³²⁻³⁶ are interpreted in order to claim that the distribution of water molecules around a central molecule is, on average, asymmetric, resulting in only two hydrogen bonds per water molecule like that shown in Figure 1.

More recently, this interpretation has been modified based on new small angle X-ray scattering data (SAXS) to suggest that water is a mixture comprised of a cluster of low-density liquid (LDL) embedded in a high density-liquid (HDL) background at room temperature and pressure, consistent with XAS and X-ray emission spectroscopy (XES).³⁶ This is a revival of the mixture models originally proposed by Roentgen³⁷ to explain, in part, water’s well known thermodynamic anomaly of having a temperature of maximum density at 4°C. Henry Frank in 1970 reviewed the experimental developments in the 1960’s and 1970’s that showed that mixture models were in conflict with known Raman and SAXS data at the time³⁸. Instead such experimental data and computer simulation³⁹ supported a homogeneous liquid environment in which every water molecule experiences the same average intermolecular force³⁸, with expected density fluctuations that deviate from the average structure. Nevertheless, Robinson and co-workers have strongly advocated a mixture model to explain the density maximum and other properties^{40, 41}. Structural polymorphism is another mixture model used to explain the anomalous properties of water emanating from a hypothetical critical point in the supercooled region⁴², which Huang et al. claim extends into and is observable at ambient temperatures and pressures.³⁶

Here we review water structure developments over the last 5 years in which we examine the various spectroscopy and scattering techniques used to probe the structure of water under ambient conditions and their interpretation using empirical models or *ab initio* studies. We show that the overwhelming scientific evidence favors the conventional view of classifying water at ambient conditions as a tetrahedral liquid, laying to rest, again, the viability of structural representations based on chains and icebergs.

2. EXPERIMENTAL TECHNIQUES USED TO PROBE THE STRUCTURE OF WATER

X-RAY AND NEUTRON SCATTERING

X-ray and neutron scattering are the most direct way in which to probe the structure of water. They provide a (long) time-averaged scattering profile that measures the differential scattering cross section per atom, or the scattered intensity⁴³, $I(Q)$

$$I(Q) = \left\langle \left| \sum_{k=1}^N b_k \exp(i\mathbf{Q} \cdot \mathbf{r}_k) \right|^2 \right\rangle, \quad (1)$$

where b_k is the scattering length of atom k , \mathbf{r}_k is the position vector of atom k , and Q is the momentum transfer for the scattering process, and the angled brackets represent an ensemble average over the system. Neutron scattering is primarily sensitive to the light nuclei in water, and by exploiting the scattering length differences between hydrogen and deuterium, all of the partial radial distribution functions (RDFs) $g_{\text{OO}}(r)$, $g_{\text{OH}}(r)$ and $g_{\text{HH}}(r)$, can be determined from a liquid neutron diffraction measurement. By contrast, X-ray scattering replaces the scattering lengths in Eq. (1) with Q -dependent atomic form factors, $f_k(Q)$, and since the scattering cross section increases with increasing atomic number, X-ray scattering is primarily sensitive to $g_{\text{OO}}(r)$.

For a homogeneous liquid, such as water, the scattered intensity per atom can be written as

$$I(Q) = I_{\text{self}}(Q) + I_{\text{intra}}(Q) + I_{\text{inter}}(Q), \quad (2)$$

where the first two terms are commonly referred to as the molecular form factor, $\langle F(Q)^2 \rangle$. The molecular form factor can be determined experimentally from X-ray scattering studies of gas-phase water⁴⁴ but it is not known for the water molecule in the condensed phase. To model the molecular form factor, the Debye approximation⁴⁵ is often used, such that

$$\langle F(Q)^2 \rangle = \sum_{ij} x_i x_j f_i(Q) f_j(Q) \frac{\sin Q r_{ij}}{Q r_{ij}} \quad (3)$$

where x_i is the atomic fraction of species i , and r_{ij} are the intramolecular distances between atom centers; at this level of approximation, the geometric framework of the water molecule is taken to be rigid, and often the individual atomic scattering factors are calculated for the isolated *unbonded* atoms. In reality, covalent bonding and solvation in the liquid phase change the charge distribution and hence the atomic form factors⁶. For example, *ab initio* simulation studies of water report that the electron distribution around a single water molecule is much changed from the gas phase, with more charge residing on the oxygen and with a more spherical distribution of charge⁴⁶. Once a model of the molecular form factor is derived, one can determine the structure factor, $S(Q)$ as

$$S(Q) = \frac{I(Q)}{\langle F(Q)^2 \rangle}. \quad (4)$$

The last term in Eq. (2) is the contribution to the total intensity due to scattering from intermolecular correlations,

$$I_{inter}(Q) = \sum_{i \leq j} (2 - \delta_{ij}) x_i x_j f_i(Q) f_j(Q) S_{ij}(Q), \quad (5)$$

where the partial structure factor, $S_{ij}(Q)$, between atom types i and j is related to the real space RDF

$$S_{ij}(Q) = 4\pi\rho \int_0^{\infty} r^2 (g_{ij}(r) - 1) \frac{\sin Qr}{Qr} dr, \quad (6)$$

where ρ is atomic density. From $I_{inter}(Q)$, we can, in principle, extract the partial structure factors and RDFs, however one needs a model for weighting the scattering from the O-O, O-H, (and H-H, ~~for which X-ray scattering is negligible~~) correlations correctly. The assumption of spherical electron density distributions around atoms, through the use of atomic scattering factors for isolated atoms, has the effect of over-weighting O-H correlation contributions to the scattering.⁶ To account for shifts in the electron density distribution of liquid water Sorenson et al.⁴⁷ have developed modified atomic scattering factors (MASFs),

$$f'(Q) = [1 + (\alpha - 1) \exp(-Q^2 / 2\delta^2)] f(Q), \quad (7)$$

where $f(Q)$ is the usual atomic form factor for an isolated atom, α is a scaling factor giving the redistribution of charge on the atom, and δ is a fitting parameter, representing the extent of

valence-electron delocalization induced by chemical bonding. The MASF formalism is an excellent model for correct weighting of O-O, and O-H correlations to reproduce the gas phase molecular form factor^{47, 48}, ~~whilst accounting and allowing~~ for modelling an increased ~~condensed phase~~ dipole moment of $\sim 2.6\text{-}3.0\text{D}$ ~~in the condensed phase to, allowing for the extraction the of~~ intermolecular $g_{\text{OO}}(r)$, and not only a molecular centres radial distribution function⁶.

Due to experimental uncertainties, and the required use of approximations in extracting RDFs from experimental spectra, the height of the first peak of $g_{\text{OO}}(r)$ has changed over the years since the original Narten and Levy experiments⁴⁹ in the 1970's. In the year 2000 however, the same peak height was determined independently from both X-ray^{47, 48} and neutron⁵⁰ scattering experiments⁵¹ (Figure 2). The water community is in agreement that the coordination number of water, measured as the area under the first peak of $g_{\text{OO}}(r)$ to the first minimum $\sim 3.4\text{\AA}$, is between 4 and 5. Without any further analysis, this would suggest that water largely retains features of the tetrahedral coordination of the ice phase, for which each water molecule is involved in four hydrogen bonds- two donors and two acceptors. However, the tetrahedral structure is further amplified by the presence of the second peak of $g_{\text{OO}}(r)$ which is dominated by tetrahedral angles, not linear angles, when the angular distribution of three oxygen vertices are considered. While the experimental scattering data does not provide us with a detailed molecular structure in the first coordination shell, the average intensity observable is consistent with real space models involving tetrahedral coordination but not chain networks as was shown in [⁵²].

X-RAY ABSORPTION SPECTROSCOPY

Following the introduction of liquid microjet technology into the soft X-ray spectroscopy experiment by Wilson et al.^{53, 54}, X-ray absorption spectroscopy (XAS) has been exploited as a method for probing the local structure of water and the hydration of solutes^{30, 31, 34, 55-62}. In XAS the energy of incident X-ray photons is such that the core electron of an atom is excited to an unoccupied electronic state. The absorption of incident radiation leads to a reduction in the measured transmitted intensity or an increase in the production of electrons or ions, yielding an intensity spectrum as a function of radiation wavelength. In water the unoccupied electronic states are sensitive to local hydrogen-bonding patterns, yielding a local environment-specific characterization of the electronic arrangement of water in the first coordination shell. Nilsson and

co-workers reported two independent studies^{30, 31} in which they used XAS to investigate the structure of the first coordination shell of liquid water. In Figure 3a we show the XA spectra of water under ambient conditions⁶³, ice and the surface of ice from Nilsson and co-workers³⁰.

In both their 2002³¹ and 2004³⁰ studies they make the observation that the X-ray spectrum of liquid water shares some similarities with that of the surface of ice, with a ‘pre-edge’ peak in intensity at ~535eV, but is very different to that of bulk ice, for which the intensity is dominated by a ‘post-edge’ region at 540-541eV. Previous analysis of the XAS spectra of the ice surface have interpreted the pre-edge peak to arise from the abundance (50% or more) of surface molecules involved in only two hydrogen-bonds (one donor, one acceptor), i.e. single donor (SD) species, while the post-edge peak of bulk ice results from double donor (DD) species in tetrahedral arrangements. Wernet et al. took linear combinations of the bulk ice and ice surface XA spectra to “fit” the liquid XA data, thereby estimating that the liquid is comprised of ~80% single donor species at room temperature (with this fraction increasing to only 85% at 90°C).³⁰ Nilsson and co-workers therefore concluded that liquid water organizes into strongly hydrogen bonded chains or rings embedded in a disordered cluster network connected by weak hydrogen bonds.³⁰

This is an unwarranted conclusion for at least two reasons. Firstly, there is an apparent lack of sensitivity of XAS to the degree of geometric distortion in the hydrogen bonding structure^{30, 59, 61, 64}. It is generally agreed upon that the spectral intensity in the pre-edge region arises from water molecules with more distorted hydrogen bond configurations than those configurations leading to intensity in the post-edge region. However, very slight distortions from the linear geometry produces the pre-edge peak⁵⁹ and without explicit *a priori* knowledge of the spectral response to the degree of geometric distortion, the similarities between the bulk water and ice surface XA spectra can only be qualitatively interpreted, i.e. that hydrogen bond deformation in bulk water is greater than in ice- which is hardly a surprise. As such, the XA spectra linear combination method employed by Wernet et al. does not and cannot quantify that liquid water has 1-2 broken hydrogen bonds⁶¹.

Secondly, the qualitative conclusions reached by Nilsson and co-workers can differ depending on which analysis method is used to determine the SD:DD ratios. In the original study by Myneni et al.³¹, the fraction of single donor species was estimated by determining the maximum fraction of the bulk ice spectrum that could be subtracted from the liquid water spectrum without introducing any strong negative features in the difference spectrum. They concluded that only 20-40% of the ice spectrum could be subtracted and that therefore liquid water was likely comprised of 60-80% broken hydrogen bonds. However, it must be noted that both the liquid water and the bulk ice XA spectra presented in this earlier work³¹ were very different than those later presented by Wernet et al.³⁰. It is now understood that the liquid water spectrum of Myneni et al. was significantly affected due to saturation effects associated with the total fluorescence yield method employed. The saturation effects artificially enhanced the pre-edge peak relative to the main edge. Furthermore, the bulk ice spectrum measured in 2002 had a much larger (and well resolved) pre-edge feature and less relative intensity in the post-edge region compared to the bulk ice spectrum in 2004. If one applies the original method used by Myneni et al. to the higher quality spectra presented by Wernet et al., we find that at least 65% of the ice spectrum can be subtracted from the liquid before any negative features are introduced in the difference spectrum, which would correspond to only 35% distorted hydrogen bonds. This is more in line with standard estimates of ~20% single donor species with a majority of water molecules involved in double donor tetrahedral coordination in the ambient liquid.

X-RAY EMISSION SPECTROSCOPY

In X-ray emission spectroscopy (XES), decay of the core-hole produced from X-ray absorption leads to emission of an X-ray photon when a valence electron falls to fill the vacant core-hole. There is some debate as to the exact nature of the information content in XES from H-bonded liquid systems (see ref. ⁶⁵ and references therein), but in general XES provides information on the selectivity of the initial absorption event, processes that occur while the molecule exists in the excited state, and the overlap between the initial, final and excited states⁶⁵. Figure 3b gives the XES spectra for liquid water, bulk ice and gas-phase water from Tokushima et al.⁶⁶

For non-resonant excitation, the XE spectrum of liquid water exhibits three main features that, broadly speaking, arise from a high emission energy non-bonding state and two lower emission

energy bonding states. These features are commonly labelled, based on the orbitals from which the valence electrons fall, $1b_1$ (non-bonding lone pair) and $3a_1$ and $1b_2$ (bonding orbitals). Recent high resolution experiments have demonstrated that the high emission energy feature (i.e. the $1b_1$ feature) has fine structure, observed as a splitting of this feature into two peaks. There has been intense debate in the literature as to the interpretation of these two peaks, with some arguing that the splitting is primarily a result of excited-state dynamics^{65, 67-70}. In contrast, Nilsson and co-workers interpret the splitting as a clear indication of ground state structure reporting on a two-state model of liquid water^{36, 66}, i.e. a mixture model of ice-like tetrahedral patches embedded in a weakly hydrogen-bonded network.

Tokushima et al.⁶⁶ argue that despite the complications imparted by excited state dynamics it remains possible to extract not only qualitative, but quantitative information regarding the distributions of hydrogen bonding configurations in water from XE spectra. Their argument derives in part from the observation that there is a clear excitation energy dependence to the observed XE spectrum^{66, 69, 71}, with resonant excitation at the pre-edge onset appearing to give an XE spectrum with no splitting of the $1b_1$ feature, while excitation at the main and post-edge yields spectra where the splitting is apparent. Furthermore, Tokushima et al. used a simple visual comparison with the gas-phase water and crystalline ice XE spectra to argue that the higher-photon energy peak of the $1b_1$ feature (termed HE $1b_1$) corresponds to distorted configurations and that the lower-photon energy peak (termed LE $1b_1$) corresponds to molecules with tetrahedral-like coordination. Then, by decomposing the observed liquid water XE spectra (in particular, the split $1b_1$ feature) into different components, Tokushima et al. conclude that distorted configurations are twice as abundant as tetrahedral configurations at room temperature, i.e. that the ratio between the area under the HE $1b_1$ peak and the LE $1b_1$ peak is 2.0 ± 0.5 at 24°C .

In a later work from the same group, to analyze small angle scattering (see below), this ratio value inexplicably changes from 2.0 ± 0.5 to 2.5 ± 0.5 at the same temperature³⁶. With this new value, Huang et al. have used the temperature dependence of this intensity ratio to determine the average energy difference between purported distorted and tetrahedral species. They showed that a plot of $\ln[I(\text{HE } 1b_1)/I(\text{LE } 1b_1)]$ vs. $1/T$ was not linear over the range 277K–363K and argue that this is a result of changes of only the distorted species with temperature. They further estimate

that the energy difference between the distorted and tetrahedral configurations increases from ~ 0.29 kcal/mol at 277K to > 1.2 kcal/mol at 363K. The room temperature values in particular are significantly lower than that derived by Smith et al. (~ 1.5 kcal/mol) from XA measurements for liquid water at temperatures less than 298K⁵⁹ and from the theoretical estimates made by Wernet et al.³⁰; this discrepancy in regards previous energy estimates was not justified or discussed by Huang et al.³⁶

However, the interpretation of the temperature dependence of the liquid water XES spectrum as providing information on the energetic difference between the distorted and tetrahedral-like configurations relies on the interpretation of the origin of the splitting in the $1b_1$ feature itself. The relative intensities and positions of the $1b_1$ fine structure depends on temperature, the incident X-ray energy and isotopic substitution.^{36, 66, 69, 72} Isotopic substitution experiments (i.e. the difference between the XE spectra of D_2O and H_2O) provide clear evidence that the XE spectrum of water is strongly influenced by excited state dynamics^{66, 69, 72}. In fact Fuchs et al.⁶⁹ note that the isotope effect is much larger than the temperature dependent differences of the water spectrum.

Furthermore, Fuchs et al. find that the intensity of the LE $1b_1$ feature (i.e. the supposedly tetrahedral feature) in D_2O is significantly less than that in H_2O even though it is generally accepted that in many ways D_2O can be considered as a cold temperature analog of H_2O and therefore, at a given temperature, might be expected to exhibit greater tetrahedrality. Taken together, Fuchs et al. argue that the LE $1b_1$ feature cannot be explained solely through a ground state structural description but must include a relatively large contribution from excited state dynamics, similar to the theoretical conclusions of Odellius^{65, 70}. Therefore any estimate of the fraction of distorted bonds relative to tetrahedral bonds in the ground state derived from the XE spectrum will not be correct. Although the observed XE spectra is entirely consistent with molecular configurations derived from traditional *ab initio* simulation methods, Odellius^{65, 70} argues that the excited state dynamics effectively masks *any* information about the structure of the ground state. Therefore XES is silent on either possibility of a uniform tetrahedral or mixture model of liquid water.

SMALL-ANGLE SCATTERING

In the experimentally inaccessible supercooled region, theory has hypothesized the existence of a second critical point, below which a dividing line separates two fluctuating liquid species of high and low density. Small-angle scattering experiments SAXS^{36, 73-78} and SANS^{79, 80} on water have mainly been concerned with determining some evidence of this critical point by measuring divergence of response functions such as the isothermal compressibility.

At temperatures far from a critical point, such as for liquid water at room temperature and pressure, the small- Q region of the scattering profile shows an increase in $S(Q)$ due to a payoff between intermolecular interactions and density. For a homogeneous fluid it measures the length scales, l_N , over which number fluctuations

$$\lim_{Q \rightarrow 0} S(Q) = \frac{\langle (N - \langle N \rangle)^2 \rangle}{\langle N \rangle} \quad (8)$$

are observable in Q -space⁸¹. An exact expression relating $I(0)$ (or the structure factor $S(0)$ using Eq. (4)) to the isothermal compressibility χ_T can be derived from thermodynamic fluctuation and kinetic theory⁴⁵

$$\lim_{Q \rightarrow 0} I(Q) = NZ^2 \rho_N k_b T \chi_T, \quad (9)$$

where ρ_N is molecule number density, Z is the atomic number, and k_b is Boltzmann's constant. Even though these density fluctuations may grow anomalously large when the fluid approaches a critical region, nonetheless thermodynamic considerations emphasize that extrapolations of $I(0)$ or $S(0)$ that conform to the limit of Eq. (9), i.e. reaching the isothermal compressibility limit, pertains to density fluctuations of a homogeneous liquid.

The decomposition of a thermodynamic property into normal and anomalous components is justified whenever "cooperative" behavior is observed and anomalous fluctuations are found to be superimposed on the 'normal' fluctuations characteristic of the property in question.⁸² To quantify the size of the "anomalous" density fluctuations in the liquid the structure factor is separated into normal $S^N(Q)$ and anomalous $S^A(Q)$ components, such that

$$S(Q) = S^N(Q) + S^A(Q). \quad (10)$$

In previous studies, $S^N(Q)$ has been estimated by either assuming that $S^N(Q)$ is independent of Q , i.e.

$$S^N = \rho_N k T \chi_T^N, \quad (11)$$

where χ_T^N is the normal component to the isothermal compressibility, or that $S^N(Q)$ can be extrapolated from $S(Q)$ at large values of Q under the constraint of reaching the $S^N(0)$ limit. In the latter case it is assumed there is no anomalous $S^A(Q)$ contribution to $S(Q)$ at large values of Q , with the choice of Q range over which $S(Q)$ is fit arbitrarily chosen. In either case, when $S^N(Q)$ is subtracted from $S(Q)$ the remaining anomalous component allows for the calculation of the Ornstein-Zernike (OZ) correlation length ξ using a Lorentzian function of the form

$$S^A(Q) = \frac{A(T)kT}{(\xi^{-2} + Q^2)}, \quad (12)$$

where $A(T)$ is a temperature specific constant. However, the Taylor expansion used to derive the OZ relation in Eq. (12) is only valid when $S(0) \gg 1$, as is expected near a critical point. The correlation length ξ in Eq. (12) becomes equivalent to l_N ~~in Eq. (8)~~ only near a critical point – and since room temperature water corresponds to a homogeneous liquid well above any hypothetical critical point in the supercooled region - the small angle region should be analyzed from the perspective of Eq. (8).

In Figure 4 we show the small-angle X-ray scattering profile of water at 25°C from a number of different studies.^{36, 73, 78} All data were placed on an absolute scale at room temperature by requiring that polynomial extrapolations to $Q=0$ converge to the isothermal compressibility limit. Using the OZ analysis on room temperature data, it was shown that similar values of ξ are obtained from $S^A(Q)$ using both S^N and $S^N(Q)$ ⁷⁸, i.e. the choice of method used to calculate the normal contribution to $S(Q)$ is unimportant. Near a critical point it is expected that the anomalous component and therefore the measured correlation length will diverge with some kind of power law dependence. However, far above the critical point, such as for ambient water, the anomalous contribution becomes smaller and smaller until it can no longer be reliably separated from normal density fluctuations.⁸³ This emphasizes the invalidity of the OZ analysis and the need to consider the meaning of the correlation length from the perspective of number fluctuations⁸³. ~~using Eq. (8).~~

3. INTERPRETATION OF EXPERIMENT USING MODELS

MIXTURE VS. CONTINUUM MODELS

Traditionally, models of water have been partitioned into two broad categories: mixture models and distorted hydrogen bond or “continuum models”^{39, 84}. Mixture models date back to the work of Roentgen in 1892 and represent water as comprising of a number of distinct molecular species.³⁷ One of the most well known is the iceberg model of water, in which ice-like clusters of water molecules sit in a sea of dissociated liquid. Robinson and co-workers^{40, 41, 85-87} have been proponents of a two species mixture model based on the ice polymorphs that are used to correlate with thermodynamic and dynamics trends of the bulk liquid. More recently the mixture model has been used to explain the anomalous properties of water emanating from the supercooled region³⁶. In particular, it underlies the main assumption of the second critical point hypothesis⁸⁸, i.e. the hypothetical existence of a liquid-liquid critical point from which a dividing line separates two fluctuating species of high and low density liquids (HDL and LDL).

Most recently, the Huang et al. SAXS study³⁶ of liquid water under *ambient* conditions made the unusual interpretation of the small-angle scattering features as arising from concentration fluctuations of two structural forms of water with different densities: a low-density liquid (LDL) and a high-density liquid (HDL), with analysis of the SAXS data estimating a feature size of the LDL species of ~13-14Å in diameter residing in a disordered HDL background. This implies that water at its compressibility limit is composed of both number fluctuations (Eq. (8)) and concentration fluctuations of two species- a mixture model.

The basic premise of mixture models at ambient conditions, i.e. that of a number of distinct molecular species, is not in agreement with a number of experimental studies and their interpretation^{38, 39, 52, 59, 61, 73, 75, 78, 79, 83, 84, 89-92}. In a homogeneous liquid such as water, every water molecule experiences the same average intermolecular force, however a model comprised of more than one species implies an inhomogeneous distribution of forces. Furthermore, studies of tetrahedral network-forming models of water^{84, 93, 94-96} have shown that for a chemically reasonable definition of the hydrogen bond, water must be well above the point at which it becomes an infinite spanning sea of associated liquid – the percolation threshold.

Whilst mixture models have been popular in analyzing a number of properties of water, they have mostly been discarded in favour of a continuum model, which dates back to the work of Bernal and Fowler¹⁴, and the distorted hydrogen-bond models of Pople⁹⁷. Continuum models represent water as a hydrogen-bond network, distorted by temperature or pressure, but not ‘broken’ nor separated into distinct molecular species as with mixture models.

SIMULATION MODELS OF WATER

Since Barker and Watts performed the first Monte Carlo calculation in 1969⁹⁸, continuum models have mostly been analyzed in the context of simulation. These early simulation models of water not only agreed with structural data, but could also account for heat capacity, dielectric constant, and the increase in volume of ice 1h upon melting.³⁹

The latest generation of simulation models typically consist of a Lennard-Jones site to represent the molecular core and dispersive interactions, and a number of rigid point-charges (differing in number, magnitude and configuration), and sometimes polarization, with the combined Coulombic interactions giving rise to directional electrostatic interactions characterized by both short and long-range features.⁸ The charge distribution of a water molecule in the bulk is shown to be symmetric in analysis of *ab initio* molecular dynamics studies⁴⁶; classical rigid fixed charge water models capture this with symmetrical hydrogen charges that balance the oxygen charge. By incorporating polarization into the model, fluctuations in the electric field of the local environment gives rise to transient asymmetric charge distributions, but the most probable observation is still symmetric hydrogen charges.¹³ Figure 5 shows that these modern “symmetric” water models, show good agreement with experimental scattering spectra; the polarizable TIP4P-Pol2 model⁹⁹ shows excellent agreement with experiment¹⁰⁰ (Figure 5a), while the fixed charge TIP4P-Ew model¹⁰¹, reparameterized under Ewald conditions to reproduce the temperature of maximum density, gives much improvement in water structure compared to the parent TIP4P water model (Figure 5b).

Some of the thermodynamic properties of water that make it different from other liquids are the maximum in density at 4°C and 1atm, a negative thermal expansion coefficient at low temperatures, a minimum in the isothermal compressibility at 46.5°C, and an anomalous increase

in heat capacity with decrease in temperature. A good model of water should be in agreement with a number of these properties as well as with structural data. Numerous models of liquid water where symmetric potentials are used fulfil this requirement. Figure 6a shows that the TIP4P-Ew model gives excellent reproduction of translational diffusion constants with temperature, and Figure 6b emphasizes that other thermodynamic trends with temperature, while not perfect, are certainly qualitatively correct.¹⁰¹ Any new structural models of water must be able to justify a large array of bulk water reference data as do these continuum tetrahedral models.

Models like TIP4P-Ew are known as “effective” potentials in the sense that they fit convenient and tractable functional forms of the molecular interactions directly to condensed phase data, i.e. they implicitly capture aspects of many-body polarization by increasing the dipole moment of the water molecule above its gas phase value, and even aspects of quantum effects are captured in the fitting to the inherently quantum mechanical experimental data. A different theoretical approach is to derive a water model completely from first principles. A recent theoretical benchmark on liquid water from such a first principles approach combines the *ab initio*-derived (but still classical) polarizable TTM2.1-F water model of Sortiris and co-workers¹⁰², with quantum simulations performed using path integral molecular dynamics (PIMD) and centroid molecular dynamics (CMD) methods^{103, 104}. Overall the TTM2.1-F model provides an overall accurate description of the water properties, especially on water cluster data, and the addition of nuclear quantum effects brings the model into better alignment with thermodynamic but especially dynamical data on liquid water. In Figure 7a we show a comparison between the experimental intensity and the simulated intensity. The combined classical/quantum model shows good agreement with experiment, which translates into partial radial distribution functions in Figure 7b that are consistent with experimental estimates of the same real space quantities.

ASYMMETRIC MODELS OF WATER

Asymmetric models of water are manifestations of mixture models that invoke a specific geometric hydrogen bonding criterion to define a “broken” hydrogen bond. Nilsson and co-workers³⁰ invoked a hydrogen-bonding cone defined around each O–H group,

$$r_{\text{OO}} < r_{\text{OO}}^{\text{Max}} - 0.00044\theta^2 \quad (13)$$

where r_{OO} is the distance of an intact H-bond, θ is the H-O \cdots O angle (in degrees), and $r_{\text{OO}}^{\text{Max}}$ is a parameter that gives the range of a cone at a straight angle (i.e., for $\theta = 0$).³⁰ Based on this geometric criterion, water molecules can be identified as existing in DD, SD, or non-donor (ND) states, depending on the value of $r_{\text{OO}}^{\text{Max}}$. Nilsson and co-workers³⁰ using density functional theory (DFT) and their original cone criterion in Eq. (13) simulated the X-ray absorption spectra for a water molecule in a very small number of artificially generated, specifically selected 11 molecule clusters of differing geometries spanning SD, DD, and ND species. It was concluded that the experimental XA spectra of liquid water could be best reproduced using predominately clusters with asymmetric SD molecules, with an average of 2.1 hydrogen bonds per molecule. When a greater proportion of DD molecule clusters were used the agreement between the calculated XA spectra and the measured liquid water spectrum was found to be worse. Furthermore, the first peak of the $g_{\text{OO}}(r)$ and $g_{\text{OH}}(r)$ radial distribution functions of these artificial clusters, weighted to give a high proportion of SD molecules, were seen to be in reasonable agreement with those extracted from neutron scattering data⁵⁰ of water under ambient conditions. In contrast, for the SPC/E model cluster of water, which is comprised of a majority of symmetric DD species with 3.3 hydrogen bonds per molecule, the calculated XA spectrum were seen to give comparably poorer agreement with experiment. Based on these model and experimental measurement comparisons, Wernet et al. concluded that even though the coordination number of water is between 4 and 5, water is only involved in two hydrogen bonds with its structure dominated by rings or chains.

However, the interpretation of the XA spectra depends critically on the hydrogen-bond definition used, [for example geometric vs. electronic as shown in \[131\]](#). It has been discussed that hydrogen bonding definitions based on one distance and one angle, such as Eq. (13), is unnecessarily arbitrary and that alternative energetic, more well-defined geometric, or quantum mechanical definitions of the hydrogen-bond are better suited for explaining IR and Raman data.⁹⁰ These alternative definitions ultimately lead to simulated observables that support conventional tetrahedral arrangements of the water liquid^{90, 105}. The cone definition also does not address the number of hydrogen bonds accepted by a molecule, although symmetry arguments with regard to the number of hydrogen bond donors can be invoked to provide an estimate of the number of hydrogen bond acceptors. Furthermore, Nilsson and co-workers later modified their

hydrogen bond criterion to be more specific, requiring an even larger asymmetry between the broken and intact hydrogen bonds; this results in very short intact bonds, very distorted broken bonds and an exclusion zone in between³⁵.

To further test the assertion that water organizes into chains, Soper¹⁰⁶ reinterpreted existing X-ray and neutron scattering data of water using empirical potential structure refinement (EPSR)^{107, 108}. In EPSR, a reference potential is perturbed to reproduce the neutron scattering profile of a given fluid. This technique is used to develop a model that gives an accurate representation of experimental scattering data, from which structural properties such as partial structure factors and RDFs can be extracted. Soper used the symmetric SPC/E model¹⁰⁹ of water as a reference potential for a symmetric model, for which the point charges have the values $q_{H1} = q_{H2} = 0.424e$ and $q_O = -0.848e$; a corresponding asymmetric reference model of water was then developed by shifting charge, such that $q_{H1} = 0.6e$, $q_{H2} = 0.0e$ and $q_O = -0.6e$. The coordination numbers of the two models were fairly similar, however the number of hydrogen bonds, calculated according to the hydrogen-bond criterion in Eq. (13) changed from 2.9 to 2.2 per molecule. The resulting structure factor of both the symmetric and asymmetric EPSR models were claimed to fit neutron diffraction data well up to $Q = 20\text{\AA}^{-1}$. As a result of the analysis, Soper¹⁰⁶ stated that both symmetric and asymmetric models of water can *probably* be made consistent with scattering data, suggesting that scattering data may not be sufficiently sensitive to distinguish between these model types. [However, later Soper revised this statement when it was found that the asymmetric model did not in fact reproduce the neutron structure factor data: a small but quite significant and unacceptable misfit of the asymmetric model to the heavy water neutron data in the Q range 3-6\text{\AA}^{-1} was later found to be the source of error¹¹⁸.](#)

Head-Gordon and Johnson⁵² have also used the asymmetric EPSR model of Soper¹⁰⁶ and the TIP4P-Pol2 polarizable model of water to examine previously reported X-ray scattering data¹⁰⁰ measured in the range $0.4\text{\AA}^{-1} < Q < 10.8\text{\AA}^{-1}$. Experimentally, the local structural order in the first coordination shell of water at 25°C is manifest as a shoulder in the X-ray intensity spectrum of liquid water at $Q \sim 3.0\text{\AA}^{-1}$. On decrease of temperature this feature is seen to sharpen, whilst on increase of temperature it is seen to “melt” out. As a result, this feature correlates empirically

with gain or loss of tetrahedral structure in water. Comparing the experimental intensity spectrum with the spectrum calculated for the asymmetric model of water, the shoulder at 3.0\AA^{-1} is seen to be diminished or absent, but is a feature clearly present in the TIP4P-Pol2 model¹⁰⁵. This suggests that a static asymmetry in hydrogen electron density when interpreting XAS data is inconsistent with other structural data that measures structural order in the liquid.

INTERPRETATION OF X-RAY ABSORPTION SPECTRA

Meaningful simulation of the XAS observable requires a reliable theoretical method for calculating core electron excited states of a water molecule residing in a statistically averaged bath of surrounding water molecule environments. Theoretical XA spectra used to interpret liquid water spectra have commonly been calculated using DFT methods, for example using the StoBe-DeMon code¹¹⁰. The DFT methods in general follow the transition potential method, but different model assumptions can be made regarding the character of the core hole that remains following excitation by the X-rays. For example, half core hole (HCH)^{30, 56, 61}, full core hole (FCH)¹¹¹ and excited state core hole (XCH)^{112, 113} approximations have all be used to calculate water XA spectra. Prendergast and Galli have shown that the choice of core hole approximation can have a strong influence on the calculated XA spectra¹¹², but no particular model is known to be more formally correct than the other model. A further consideration is that the transition potential DFT methods only provide “stick” spectra (i.e. energy and oscillator strength), and therefore to allow for comparison with observations, the transitions must be artificially broadened. There is no agreed upon method for choosing a broadening scheme to describe liquid water.⁶¹

The theoretical DFT calculation requires a structural model of the liquid. In their 2004 study, Wernet et al.³⁰ determined best fit XA spectra by adjusting the percentages of DD, SD and ND water molecules from a small number of 11 molecule clusters. Only 14 configurations total were used: 5 DD, 8 SD and 1 ND³⁰. These 14 configurations were not obtained from MD snapshots, but were instead ‘systematically’ (as opposed to randomly) generated by artificially moving groups of molecules surrounding the central molecule. Wernet et al. report that the observed XA spectrum was best reproduced using a ratio percentage of DD:SD:ND of 10:85:5, corresponding to an average of 2.1 hydrogen bonds per molecule, counting both donor and acceptor hydrogen

bonds. If the DD:SD:ND ratio from a SPC/E simulation of 70:27:3 was instead used (corresponding to 3.3 hydrogen bonds per molecule), relatively poor model/measurement agreement was obtained. Based on this analysis it was suggested that water is, on average, only involved in two hydrogen bonds (one donor + one acceptor), with its structure therefore dominated by rings or chains rather than the traditionally accepted tetrahedral structure.

The methods used by Wernet et al. to generate the XA spectra using DFT and the choice of water cluster geometries have been criticized by Smith et al.⁶¹, who showed that the XA spectra of molecules that exist within the same class, e.g. single donors, can vary dramatically depending on the local environment. Thus, it is impossible to generate meaningful comparisons in spectra based on hydrogen-bonded classes with so few configurations. Instead, Smith et al. showed that when a much larger *random* sampling of individual configurations was considered (60 DD, 60 SD and 30 ND) the resulting average, weighted XA spectrum of water assuming the DD:SD:ND ratio of 10:85:5 from Wernet et al. fared no better, and possibly slightly worse, than a traditional tetrahedral bonding configuration of 80:10:10 in reproducing the experimental spectrum. Furthermore, Smith et al. showed that model/measurement comparison is further complicated by there being a dependence of the absolute results on the density functional used in the calculation of the individual XA spectra, and on the specific choice of a spectral broadening scheme. As a consequence, current theoretical models for XA are insufficiently developed to draw *quantitative* conclusions about the structure of water from calculated XA spectra, and even *qualitative* conclusions are subject to these computational limitations.

INTERPRETATION OF SMALL ANGLE SCATTERING

The small- Q region of water is not easily amenable to simulation studies due to the large box size required to reach this region. One of the first investigations of the size of density fluctuations in water was by Geiger and Stanley⁹⁵ who calculated the radius of gyration of four-coordinated clusters $R_{g,4}$ in a 216 molecule ST2 simulation of water at -15°C using

$$R_{g,4}^2 = \frac{1}{S} \sum_{i=1}^S (\underline{r}_i - R)^2 \quad (14)$$

where \underline{r}_i are the oxygen atom positions and the index i labels the atoms in a cluster of size s . They calculated a maximum value between $R_{g,4}^{max} \sim 2.2\text{\AA}$ and 3.2\AA ($D_{s,4}^{ma} \sim 5.6\text{\AA}$ and 8.3\AA).

More recently, Molinero and Moore¹¹⁴ have developed a monoatomic model of water (mW) model that represents a water molecule as a single particle with tetrahedral interactions that mimic the effect of hydrogen bonds. The mW model does not have hydrogen atoms or electrostatic interactions making it less expensive than traditional simulation models of water, while still being able to reproduce qualitatively, and for some properties quantitatively, the structure of water, ice, and the thermodynamic and dynamic anomalies of water. Using this model Moore and Molinero¹¹⁵ have investigated the small- Q region to $Q \sim 0.1\text{\AA}^{-1}$ in the temperature range $-88^\circ\text{C} < T < 72^\circ\text{C}$ for system sizes of $N > 250,000$ molecules in boxes of side $\sim 20\text{nm}$. They determined the presence of a low density species based on four-coordinated waters whose largest radius of gyration was calculated using Eq. (14). A constant average value of $R_{g,4}^{max} = 9\pm 1\text{\AA}$ was found for $T > 27^\circ\text{C}$, whilst for $T < 27^\circ\text{C}$, $R_{g,4}^{max}$ was seen to increase with decreasing temperature to a value of $\sim 24\text{\AA}$ at $T \sim -43^\circ\text{C}$.

However, on explicit calculation of small angle scattering spectra using Eq. (6), Moore and Molinero found that on decreasing temperature, the mW model showed no discernible increase in $S(Q)$ at small Q at any temperature (Figure 8), because there is no significant density contrast between the ‘low’ and ‘high’ density species within the mW model. Instead, Moore and Molinero analyzed their data to measure the correlation length of four-coordinated clusters, i.e. water molecules that are strictly four-coordinated up to a radial cutoff distance r_c . The resulting $S_4(Q)$ did show a pronounced increase at low Q (but the degree was very sensitive to the value of r_c used). Using Eq. (12) Moore and Molinero calculated the correlation length for $S_4(Q)$ (not $S(Q)$), finding that $\xi_4=1.6\text{\AA}$ at room temperature changes to $\xi_4 = 3.3\text{\AA}$ at -88°C . These correlation lengths based on $S_4(Q)$ are structural and not related to the density fluctuations of a SAXS experiment that reports on $S(Q)$. Nonetheless, they are small values at any temperature.

Huang et al.³⁶ have used the SPC/E model of water to simulate the small- Q region over the temperature range $5^\circ\text{C} < T < 67^\circ\text{C}$, and they observe no increase in $S(Q)$ at small Q . However, it is known that the isothermal compressibility trend with temperature for the SPC/E model of water is not in qualitative agreement with experiment¹¹⁶. Clark et al.⁷⁸ have shown that the tetrahedral network forming TIP4P-Ew model of water does reproduce the increase in $S(Q)$ at

small Q , consistent with small-angle X-ray scattering data on ambient liquid water taken at third generation synchrotron sources^{36, 78}. In recently reported work, they performed large 32,000 water molecule simulations using the TIP4P-Ew model, in which they measured a correlation length of $\sim 2.0\text{-}3.0\text{\AA}$ at room temperature⁷⁸.

In summary, for temperatures far above the supercooled state, all recently reported SAXS data for water measure density fluctuations that conform to the trend in isothermal compressibility with temperature, as expected for a single phase liquid. The disparity in the reported correlation length values at room temperature among different models and experiments arises from the ambiguity in clearly distinguishing the small anomalous component from the normal fluctuations that dominate at temperatures far from the critical point. Any inhomogeneity is therefore only “observable” on some non-macroscopic length scale, and are simply interpreted as deviations from the average density, i.e arising from stochastic fluctuations. Note that these non-macroscopic length scales are all consistently small, 1.2-3.1 \AA , in all reported experiments and simulations.

REVERSE MONTE CARLO

Pettersson and co-workers have recently used reverse Monte Carlo (RMC) modelling to fit symmetrical and asymmetrical models of water^{33, 117} to both experimental scattering^{100, 118} and infrared (IR)/Raman^{119, 120} data supplied in the form of constraints. Additional geometric constraints were enforced in the RMC procedure by altering $r_{\text{OO}}^{\text{Max}}$ to create two ensembles of structures; one in which tetrahedral or DD species are maximized, and one in which the number of asymmetric or SD species are maximized. Leetmaa et al. claim to reproduce the scattering and vibrational data equally well by both model types, thereby concluding that scattering, IR and Raman spectra cannot be used to provide proof of tetrahedral or asymmetric liquid water structure.³³ However, the first peak of the extracted RDFs for the primitive RMC models are significantly shorter and broader than those extracted independently from other scattering experiments, while an unphysical peak is observed in the OH correlation³².

There are a number of concerns regarding the methodology employed in this analysis. Firstly, a density of $\sim 0.9\text{g/cc}$ was used in the RMC simulations reported in [33]- which is a very low

density to describe ambient water. Whilst the cone definition used to define an intact hydrogen bond (Eq. (13)) was modified from that reported in previous studies and required 7 pages in supplementary material to describe what defined a SD and DD species.³³ It appears that multiple cones were used with the range of $2.83\text{\AA} < r_{\text{OO}}^{\text{Max}} < 3.3\text{\AA}$ to generate the asymmetric SD model- which the authors acknowledge is a narrower range than they used in their original study³⁰ - and $3.0\text{\AA} < r_{\text{OO}}^{\text{Max}} < 3.3\text{\AA}$ for the DD model. The authors have therefore confirmed that the DD model reproduces the experimental data, but actually never investigated a SD model consistent with their other studies.

These works are also misleading in regard to the experimental data that was used. The stated use of experimental Raman and IR data by Leetmaa et al³³ are actually *models* of the electric field distribution that “show a correlation” with *quantum mechanical models of clusters* of a local uncoupled OH stretch. Furthermore, the X-ray scattering data of Hura and co-workers that was originally reported in [48] and which is reproduced in Figure 9a, was changed in the work of Leetmaa et al.³³, as seen in Figure 9b. The first two peaks of the structure factor in the original experimental work by Hura and co-workers have different amplitudes; note that in Figure 9a other previous and independent scattering experiments and simulation using the SPC/E model have the same qualitative features. In Figure 9b, Leetmaa et al have inadvertently used renormalized experimental data of Hura and co-workers (normalized using atomic form factors as opposed to the molecular form factor of the original study), so that the first two peaks now have the same amplitude. It is apparent that they did not use the new normalization procedure for the SPC/E data. The importance of this is that they argue that simulation models such as SPC/E generate a sharp first peak in $g_{\text{OO}}(r)$ due to asymmetry in the first two Q -space peaks, while symmetric Q -space peaks typically reduce the height and broadens the first real space peak. It is clear that Leetmaa et al.³³ and Wikfeldt et al.¹¹⁷ have poor understanding and control of the structure factor data, and therefore the resulting inconsistencies negate the legitimacy of conclusions drawn from these studies.

The primitive RMC approach as developed in [33, 117] is a retrograde step in water structure analysis. In early interpretations of liquid structure data, “pure” RMC methods were employed so the analysis would not be tainted by assumptions or input from a theoretical model. The hope

was that sole reliance on the experimental structure factor data would lead to a converged and correct three-dimensional structure of the liquid. In fact, the higher order angular correlations were poorly described by the limited radial experimental constraints. This is why advanced RMC methods such as ESPR¹⁰⁸ were developed in the first place- the reference potential provides a physical starting structure of the three-dimensional liquid that is perturbed to reproduce experimental structure factors without artifacts of unphysical higher order correlations.

4. RELATION BETWEEN STRUCTURE AND THERMODYNAMICS

As stated by Pettersson and co-workers³², the structures resulting from RMC are not necessarily correct or even thermodynamically accessible. However, thermodynamics is an important constraint on viable structural models of the liquid that is largely ignored by Nilsson and co-workers. Head-Gordon and Rick analyzed the thermodynamic consequences of chain networks using three different modified water models that exhibit a local hydrogen-bonding environment of two hydrogen-bonds, including the asymmetric EPSR model.¹³ They found that bulk densities, enthalpies of vaporization, heat capacities, isothermal compressibilities, thermal expansion coefficients, and dielectric constants, over the temperature range of 235K-323K, were in poor agreement with experiment, and that water models that assume a predominance of SD species behave in most respects as normal liquids. The asymmetric EPSR model was found to be a gas at 1atm, and at ambient water densities of 1g/cc is at a pressure of ~10,000atm.¹³ This is also evident from its positive free energy for water molecule insertion, indicating that the asymmetric EPSR model is thermodynamically unstable.¹³

In going from ice to liquid, the validity of the Wernet et al. picture must account for the energetics of converting two strong hydrogen bonds per molecule in ice (two to avoid double counting) to one strong and one “weak” hydrogen bond per molecule in the liquid. Given that the heat of fusion of ice is 6.01kJ/mol, then the following thermodynamic relation should hold

$$2\varepsilon_s + 6.01 = \varepsilon_s + \varepsilon_w \quad (15)$$

where ε_s is the energy of a strong hydrogen bond, and ε_w that of a weak bond (the pressure-volume terms for water and ice are negligible at ambient pressure). Assigning the conventional value of 23kJ/mole to strong bonds¹⁵, this yields a value of 17kJ/mole or 4.1kcal/mole for the strength of “weak” hydrogen bonds advocated by Wernet et al. This value is in fact completely within the

normal range of hydrogen bond strengths sampled in liquid water as a result of thermal fluctuations¹⁵. Entirely similar conclusions can be reached by noting that the ratio of water's heat of fusion to its heat of sublimation at the triple point is ~ 0.11 , showing that the vast majority of hydrogen bonds remain energetically intact upon melting.

5. CONCLUDING REMARKS

In this review we have described what is known about liquid water structure, with a primary focus on ambient water and new structural experiments, simulation, and *ab initio* theory results over the last 5 years. We summarize these results as follows.

The radial distribution functions extracted from independent wide-angle X-ray and neutron scattering experiments and analysis yield a coordination number for water of between 4 and 5, with well-defined peaks in the RDFs that imply a tetrahedral coordination similar to that of ice.^{6, 47, 48, 50, 100} The application of an Ornstein-Zernike analysis to regions far away from the critical point is invalid due to a negligible anomalous contribution to the structure factor. In these regions the correlation length reports on the size of a window in which density fluctuations corresponding to stochastic number fluctuations can be observed, rather than on the length scales of 'concentration fluctuations' between different structural species. The XA spectrum of liquid water appears to be more similar to that of the surface of ice rather than bulk ice^{30, 59, 61}; however, without *a priori* knowledge of the spectral response to a distorted hydrogen bond this only tells us that hydrogen bonds in liquid water are more distorted than in ice⁶¹, which is already well known. Furthermore, the energy required to distort a hydrogen bond, experimentally derived from X-ray absorption spectroscopy, is consistent with tetrahedral network forming models of water such as the ST2 model of water.^{59, 64} Finally, theoretical techniques are not sufficiently accurate enough to calculate XA spectra reliably^{32, 61}, while XE spectra may be reporting on excited state dynamics as opposed to ground state structure. While the XA and XES spectroscopic observables may be unable to distinguish between qualitatively different models of water, they certainly are always consistent with a (distorted) tetrahedral network model.

Recent generation effective potentials for water, which assume, on average, a symmetrical distribution of charge across the hydrogen atoms and form a continuous tetrahedrally-

coordinated network, are in good agreement with a wide range of experimental data. For example the TIP4P-Ew¹⁰¹ and TIP4P-Pol2⁹⁹ models provide good agreement with experimental scattering data, such as the oxygen-oxygen RDF independently extracted from X-ray scattering and neutron scattering studies of water^{51, 101}, and the small-angle scattering region⁷⁸. Such models are also in qualitative agreement with IR and Raman spectra.^{89, 90} Furthermore, they reproduce a number of thermodynamic and dynamic properties, such as the maximum in density and the minimum in isothermal compressibility with temperature, translational diffusion constants, vapor-liquid equilibrium properties, free energies of small, non-polar molecules, and are in qualitative agreement with the phase diagram of water.^{99, 101, 121, 122} Early ground breaking *ab initio* simulations of liquid water^{46, 123-125} are realizing continued improvement based on combining good classical simulation models with electronic and nuclear quantum methods, or new stand alone *ab initio* molecular dynamics, that show very good agreement with a range of thermodynamic and dynamical experimental observables^{100, 104, 126, 127}. While theoretical models and methods are not perfect, the point is that they are very good in reproducing a host of reference data beyond structure that make them a robust and reliable companion to many types of experimental studies.

Models of hydrogen-bonding or local water organization, which assume, on average, an asymmetric distribution of charge across the hydrogen atoms to form strongly hydrogen-bonded chains or rings perform poorly for a number of experimental properties. An asymmetric empirical potential structure refinement (EPSR) model of water ~~gives good agreement to experimental scattering data, however, it~~ yields a $g_{OO}(r)$ of water with an unphysical peak that corresponds to a linear arrangement of three oxygens^{52, 106}, and other chain network models are devoid of a second peak in their RDFs¹³. Furthermore, subsequent work has shown that the asymmetric model performs poorly on neutron data taken on D₂O¹¹⁸, and the model does not provide a good fit to the intensity data of wide-angle X-ray scattering spectra.⁵² At ambient temperature and density the EPSR asymmetric model has a pressure of 10,000atm and captures none of waters anomalous thermodynamic properties.¹³ The calculated Raman spectrum for this model also yields a bimodal distribution qualitatively different to the unimodal distribution observed in experiment^{32, 61}.

The reasons for poor agreement stem, in part, from the arbitrary definition of a hydrogen-bond (Eq. (13)) that enforces an ice-like definition of a double donor, symmetric species to arrive at an estimate for the liquid in which ~80% of water molecules are classified as asymmetric, single donors. The changing definition of a hydrogen bond by Nilsson, Pettersson, and co-workers over the span of 5 years of studies clearly indicates that a single definition for a dominant SD species is incapable of describing a host of experimental data adequately. Kumar et al. showed that theoretical calculation of various vibrational spectroscopy observables were consistent with a 27% fraction of HOD molecules that are single donor species, and if this fraction were significantly higher, the resulting vibrational line shapes would not be compatible with experiment^{89, 90}. Models that exhibit local hydrogen-bonding environments dominated by single donors show poor agreement with experimentally measured thermodynamic and dielectric properties, and behave similarly in most respects to normal liquids.¹³ Basic thermodynamic arguments show that the energetics of “weak” hydrogen bonds are in fact entirely consistent with thermally distorted but intact hydrogen bonds of a predominately symmetric DD liquid.

The maturation of water science in the late 1970's^{8, 15} solidified the acceptance that the structure of liquid water under ambient conditions is, on average, tetrahedral. On the balance of available evidence, from experiment and theory, this is still the case today. This classification informs our reference state for comparison against normal liquids, changes in water properties as we traverse more extreme regions of the phase diagram, or alterations of its local environment with the addition of solutes or interfaces. The question for participating researchers in water science is whether it is helpful to our field to recycle controversies or revisit discredited concepts and ideas, as if we know less about water than we did 30 years ago. It seems evident that our field will only be able to pursue stimulating and deep questions about what is not known about water and its perplexing properties, for example in the supercooled region or for real aqueous mixtures, if we are not deterred from what we do know about bulk water at ambient conditions.

ACKNOWLEDGMENTS. GNIC and THG thank the NSF Cyberinfrastructure program, and GLH thanks the Department of Energy, for support of the work presented here. We also thank the National Energy Research Scientific Computing Center for computational resources. THG thanks Jose Teixeira and Alan Soper for helpful discussions. We thank the reviewer for the

thermodynamic argument about hydrogen-bond strength. We also thank Valeria Molinero and Francesco Paesani for the data presented in Figures 7 and 8.

REFERENCES

FIGURE CAPTIONS

Figure 1. *One proposed hydrogen-bonded network model for polywater.* Lippincott and co-workers²¹ suggested that the spectral features of the highly viscous water was composed of polymeric hydrogen bonded chains between molecules. Reproduced with permission.

Figure 2: *The oxygen-oxygen radial distribution function (RDF), $g_{oo}(r)$, of water under ambient conditions extracted from experimental X-ray scattering data.*⁴⁸ The area under the first peak to $r \sim 3.4\text{\AA}$ gives a coordination number of between 4 and 5.

Figure 3: *The experimental X-ray absorption (XA) and X-ray emission (XE) spectra of various phases of water.* (a) The XA spectra (or X-ray Raman spectra) for liquid water, the ice surface, the ice surface after termination by NH_3 , and bulk ice. Adapted from Wernet et al.³⁰ (b) The XE spectra for gas-phase water, liquid water at various temperatures, amorphous ice and bulk ice. Adapted from Tokushima et al.⁶⁶

Figure 4: *The experimental small-angle X-ray scattering profile of water at 25 °C.* Clark et al.⁷⁸ (black), Huang et al.³⁶ (orange), and Bosio et al.⁷³ (magenta). (*Inset*) Ornstein-Zernike analysis of small-angle X-ray scattering data. A comparison of the Lorentzian fits calculated using $S^N(Q)$ dependent on Q (---) and S^N constant over the Q -range (—) is made to the experimental data of Clark et al. (black) and Huang et al. (orange and red) anomalous structure factor component $S^A(Q)$ data at 25°C. In both the triangle is the estimated zero-angle scattering⁷⁸.

Figure 5. *Comparison of the experimental X-ray scattering profile of water at 25 °C with that calculated using modern “symmetric” models of water.* (a) Experiment¹⁰⁰ (black) and TIP4P-Pol2⁹⁹ (gray) Reproduced with permission. (b) Experiment¹⁰⁰ (black), TIP4P¹²⁸ (red) and TIP4P-Ew¹⁰¹ (blue).

Figure 6. *Comparison of the experimental (—□) dynamic and thermodynamic properties of water with those calculated using the TIP4P-Ew model of water (---○), as a function of*

temperature.¹⁰¹ From top to bottom: translational self-diffusion coefficient D , isobaric heat capacity c_p , isothermal compressibility χ_T , and thermal expansion coefficient α_p . Adapted from Horn et al.¹⁰¹

Figure 7. (a) The X-ray scattering profile and (b) extracted O-O radial distribution function of water at 25 °C from experiment (black) and calculated using the classical TTM2.1-F model¹⁰² of water (blue) and the TTM2.1-F model combined with quantum simulations¹⁰³ (red).

Figure 8. Structure factor data for the mW model.¹¹⁵ The total structure factor $S(Q)$ at 300K (black line) and 210K (red line with circles), for which no increase at small Q is observed in the simulations. The remaining curves are for different temperatures (210K to 300K) of $S_d(Q)$ for $r_c = 3.5\text{\AA}$. Reproduced with permission.

Figure 9. (a) Structure factor ($h_{OO}(Q)$) from previously reported experiments and simulation on liquid water at room temperature. Narten and Levy^{49, 129} (green dot-dash line); Soper, Bruni, and Ricci¹³⁰ (red line); Hura et al. (black line); SPC/E (blue dashed line). The curve for Narten and Levy is $H_M(Q)$ taken from their paper; the curve for Soper et al. is taken from applying a Fourier transform to the $g_{OO}(r)$ given in [¹³⁰]. (b) Structure factor ($S(Q)$) of the inconsistently normalized ALS and SPC/E data by Pettersson and co-workers^{33, 117}. Reproduced with permission.

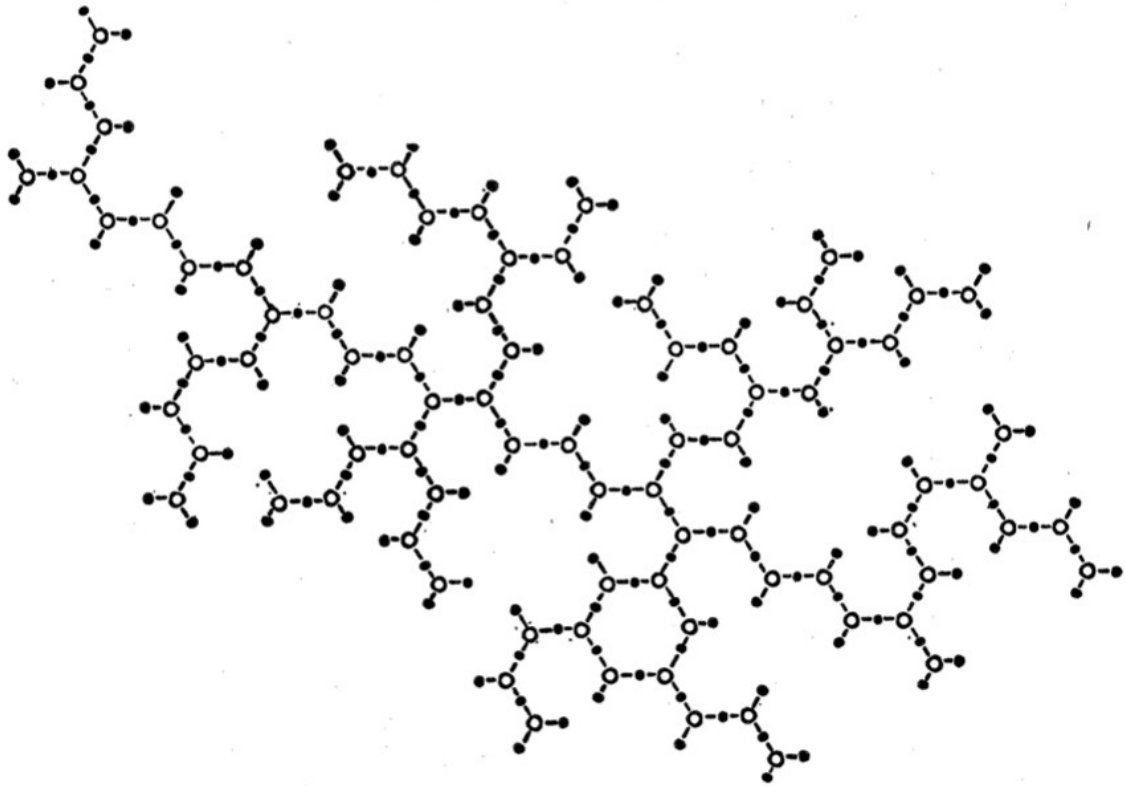


Figure 1. Clark and co-workers

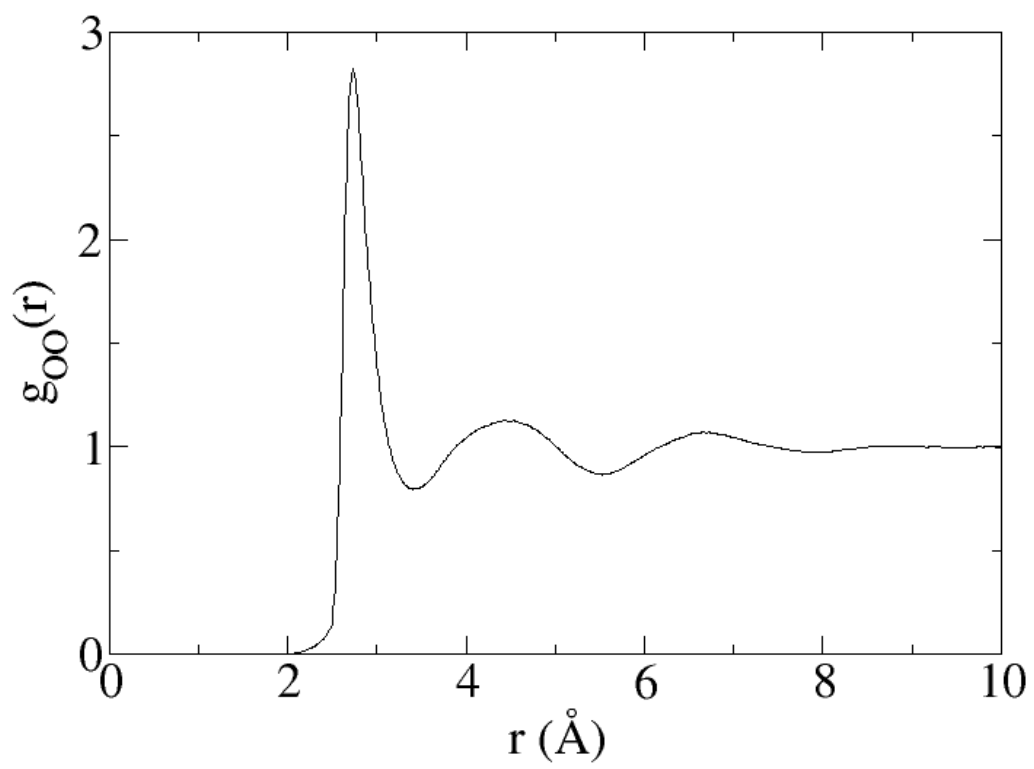


Figure 2. Clark and co-workers

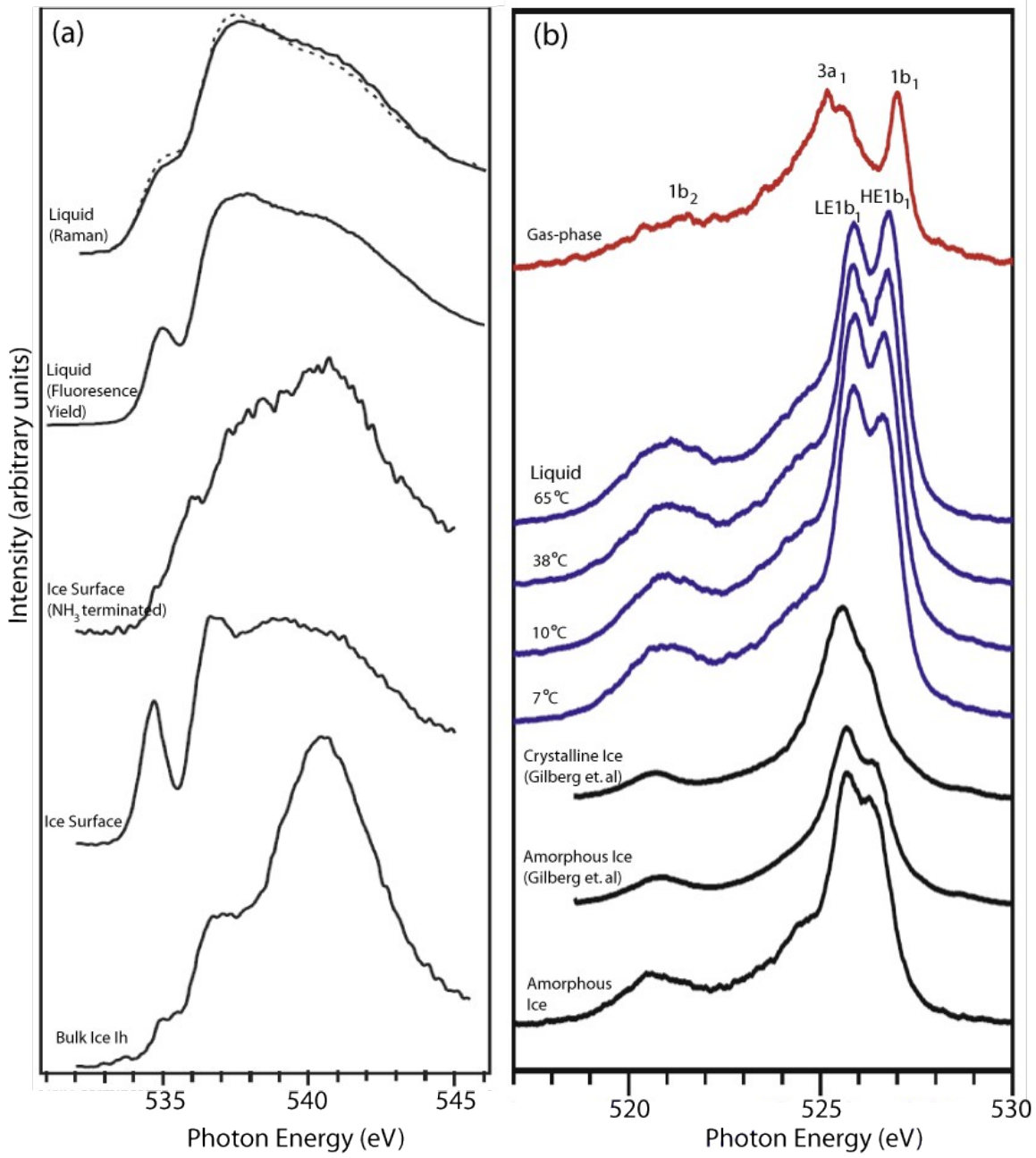


Figure 3. Clark and co-workers

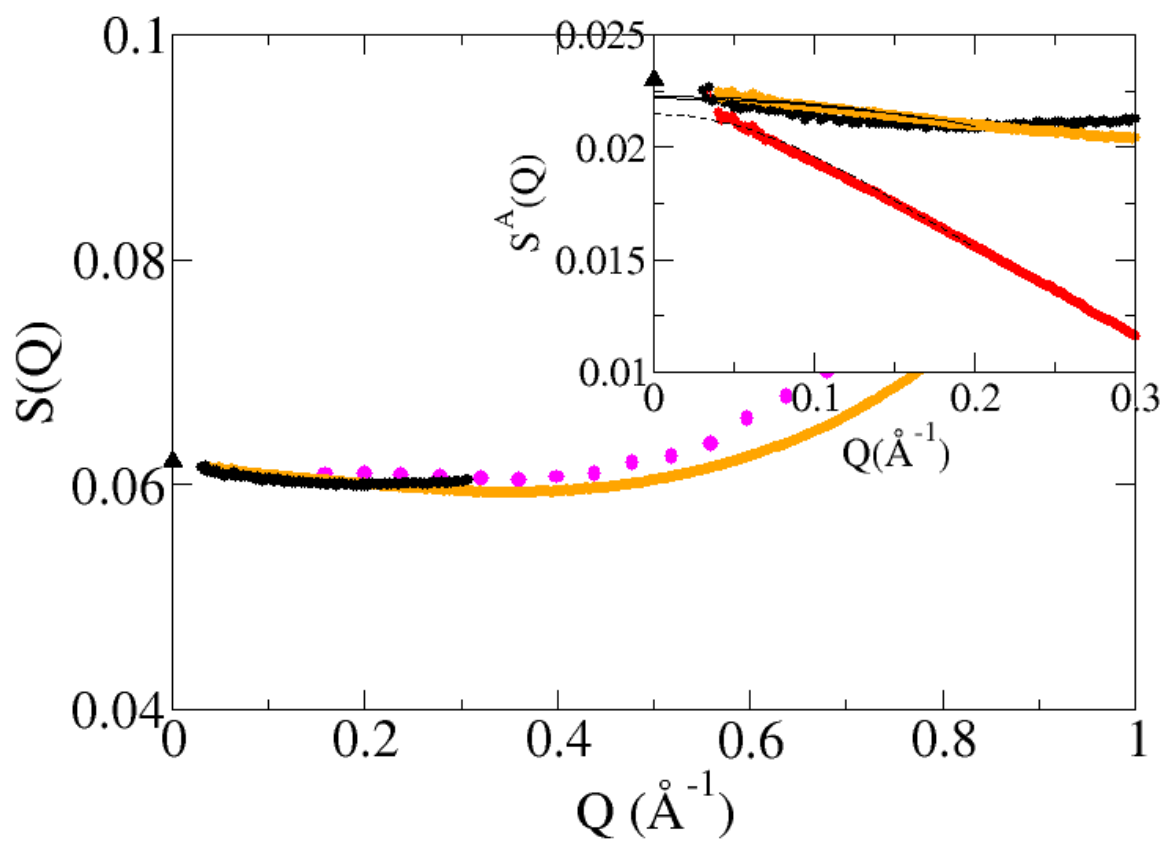


Figure 4. Clark and co-workers

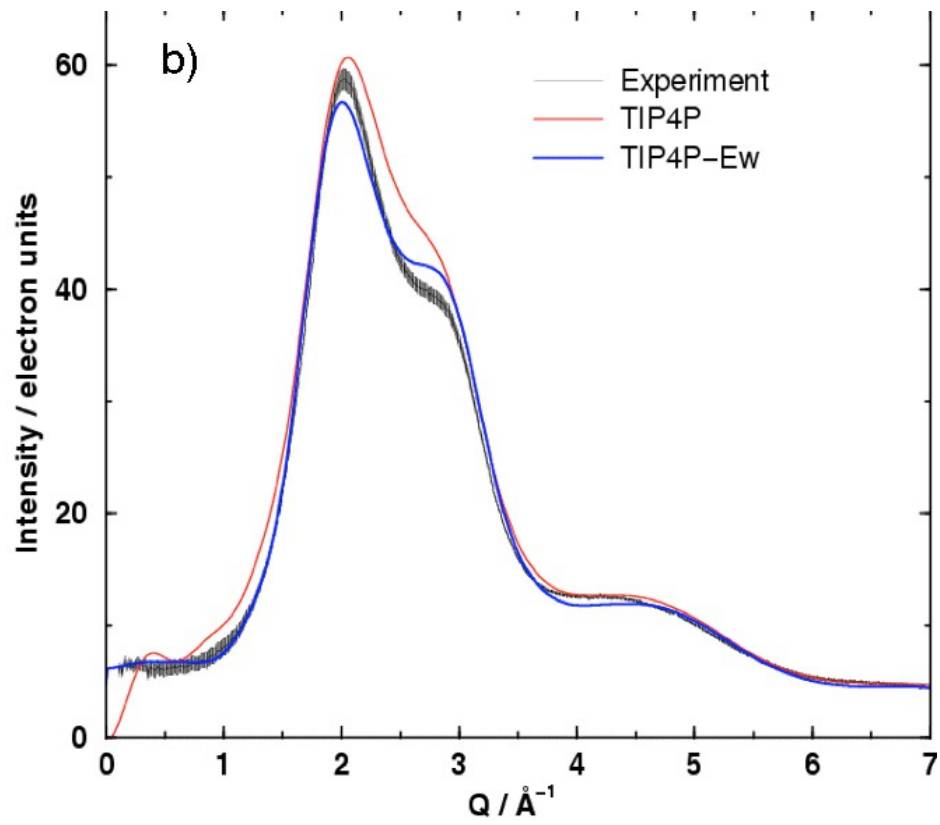
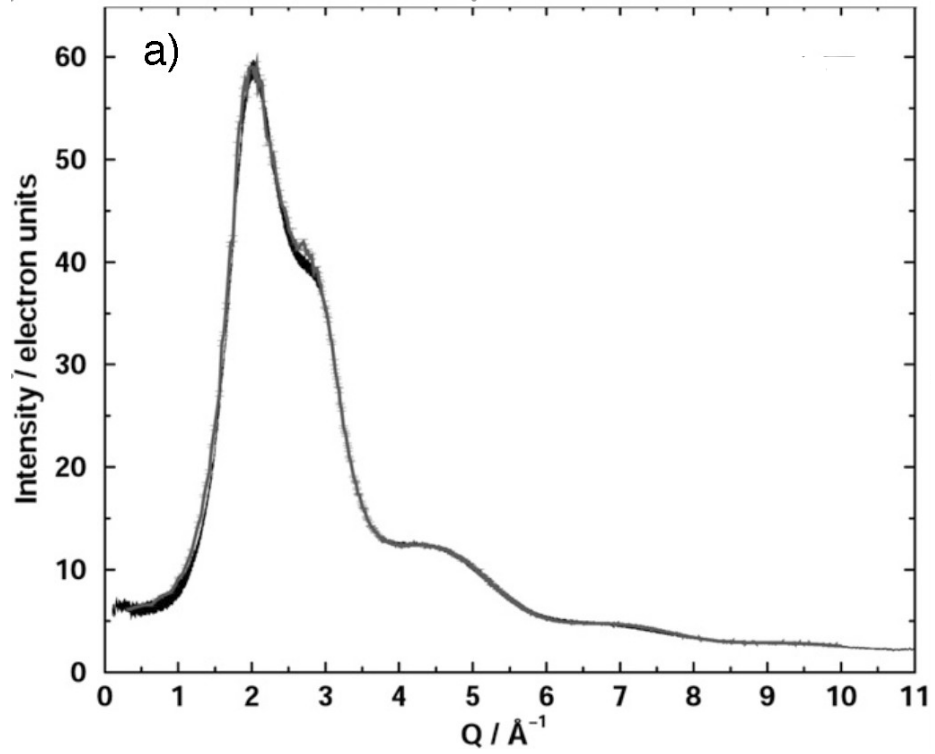


Figure 5. Clark and co-workers

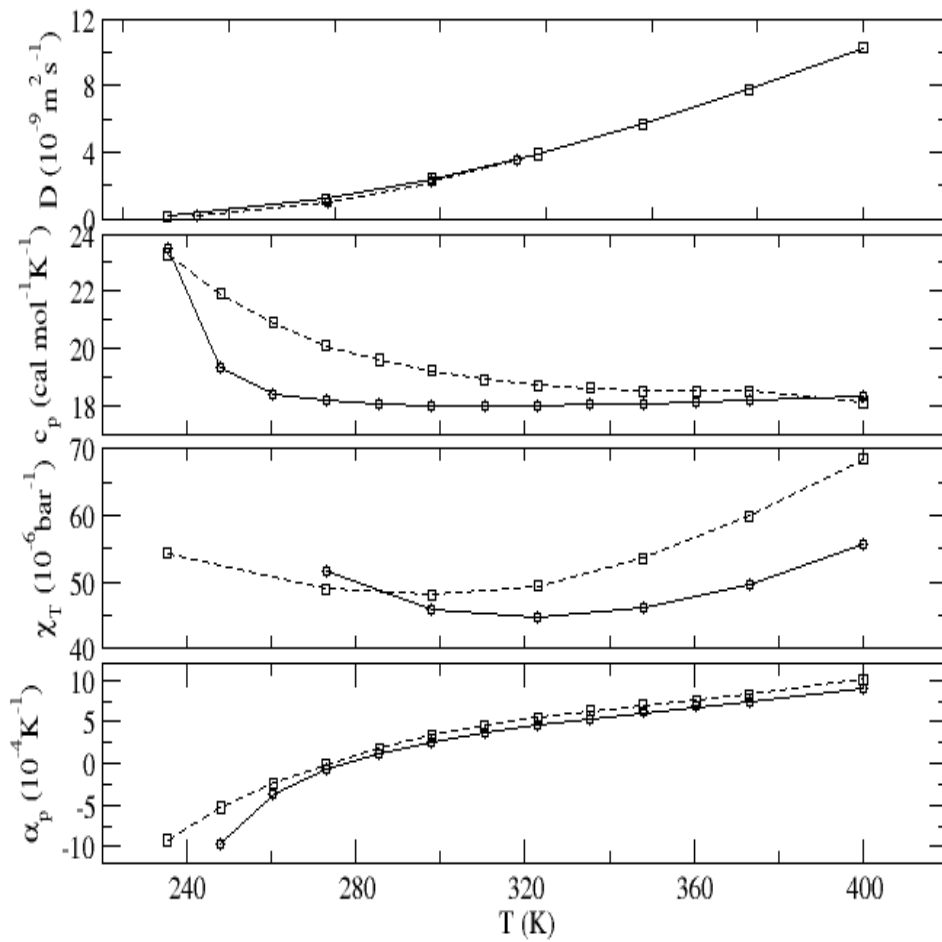


Figure 6. Clark and co-workers

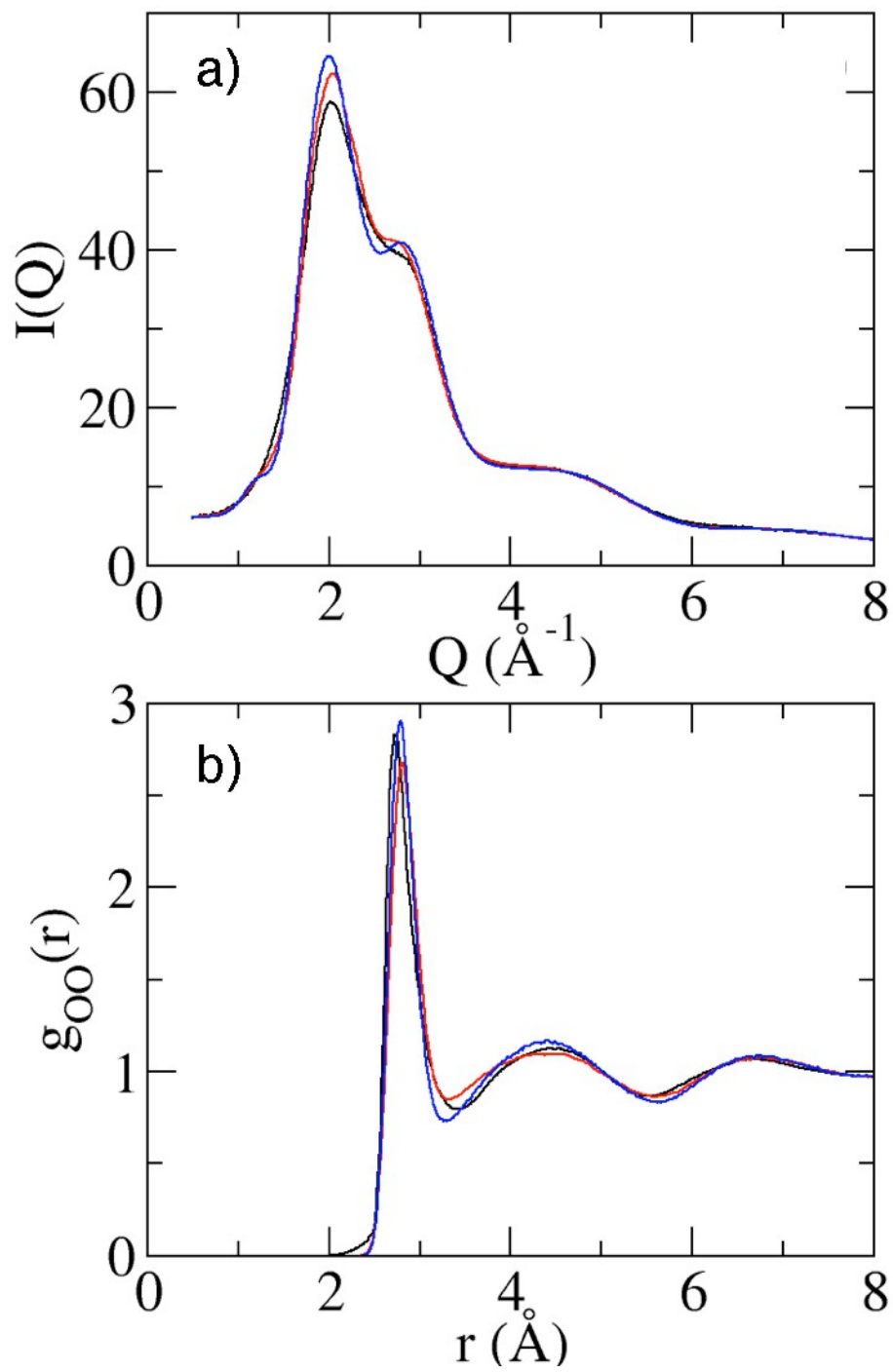


Figure 7. Clark and co-workers

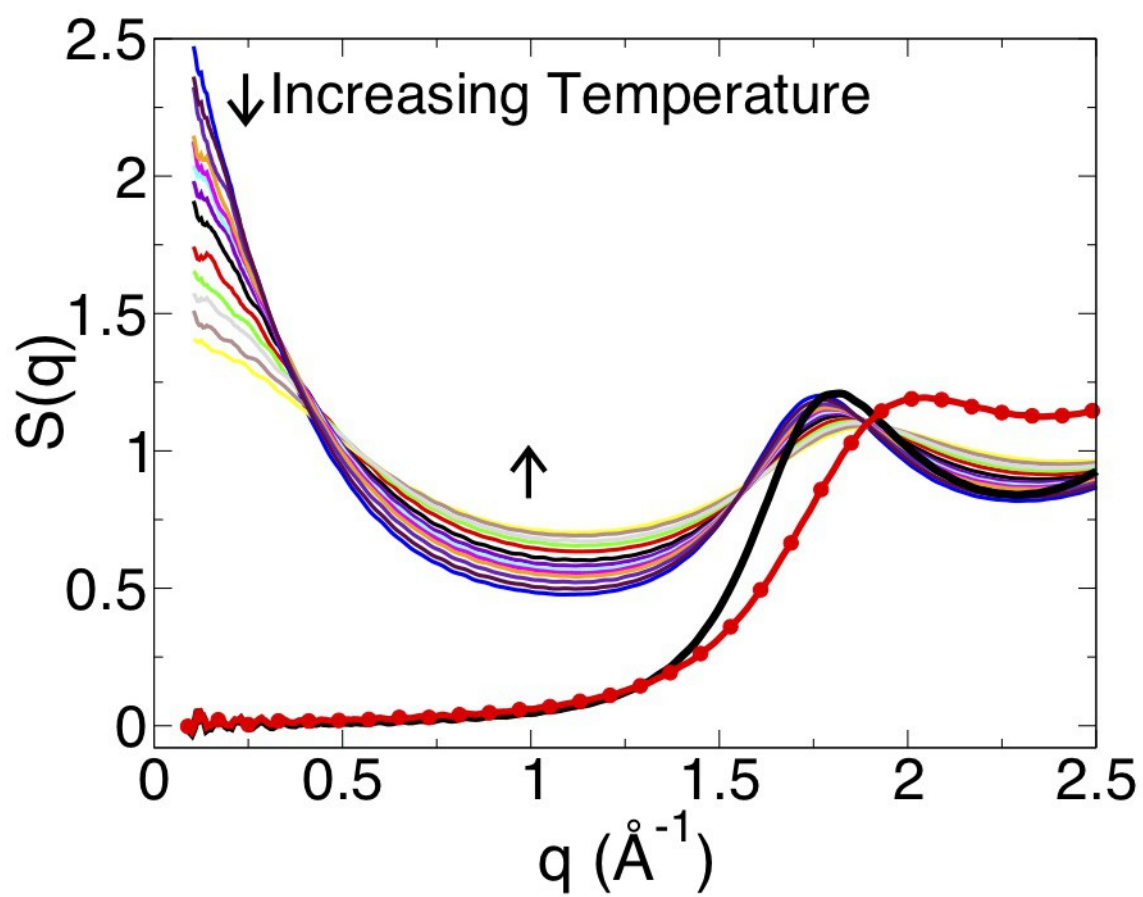


Figure 8. Clark and co-workers

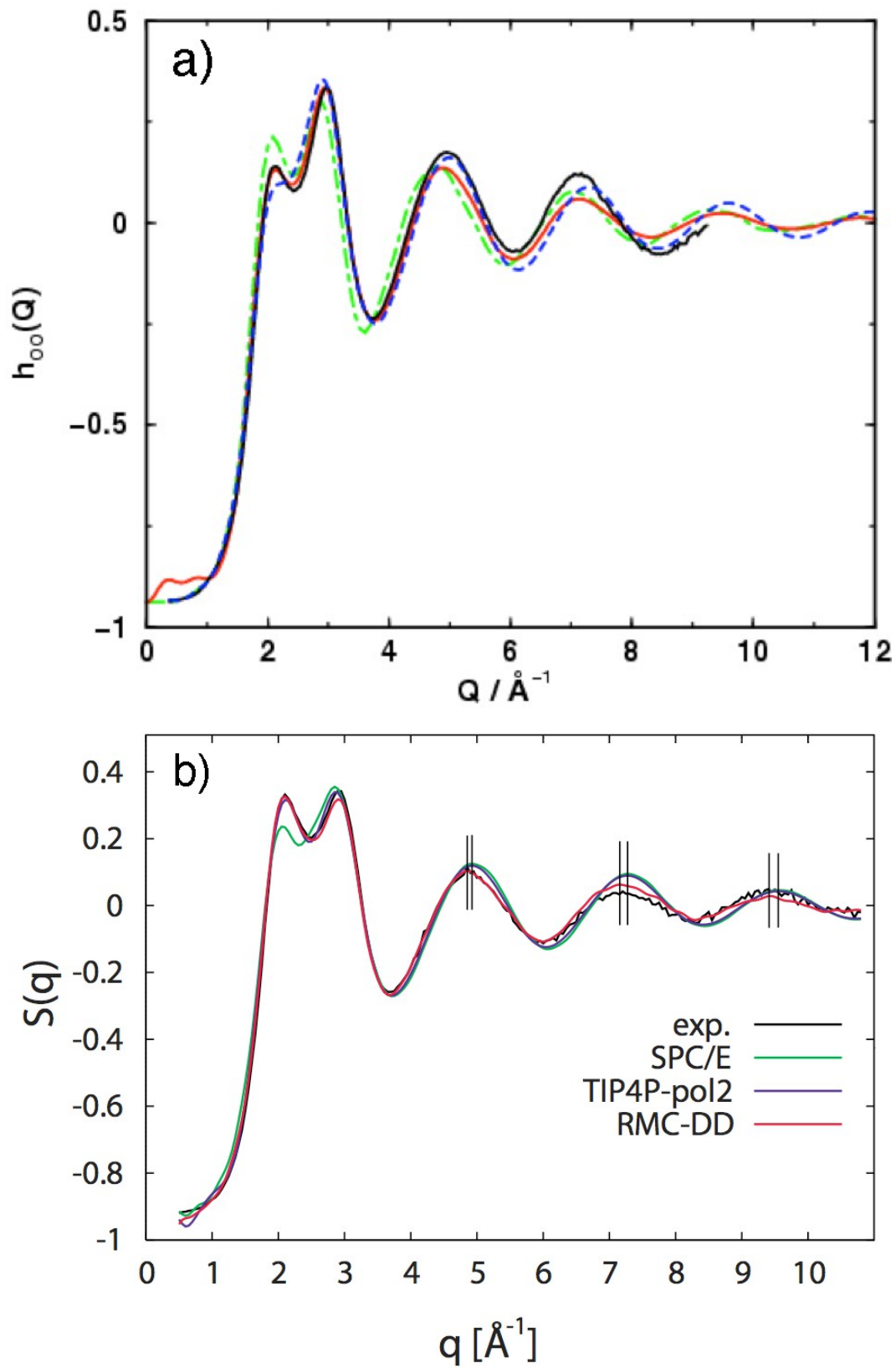


Figure 9. Clark and co-workers